Measured and Calculated Losses in a Model Dipole for GSI's Heavy Ion Synchrotron

M. N. Wilson, M. Anerella, G. Ganetis, A. K. Ghosh, P. Joshi, A. Marone, C. Muehle, J. Muratore, J. Schmalzle, R. Soika, R. Thomas, P. Wanderer, J. Kaugerts, G. Moritz, W. V. Hassenzahl

Abstract--**The new heavy ion synchrotron facility proposed by GSI will have two superconducting magnet rings in the same tunnel, with rigidities of 300T·m and 100T·m. Fast ramp times are needed. These can cause problems of of ac loss and field distortion in the magnets. For the high energy ring, a 1m model dipole magnet has been built, based on the RHIC dipole design. This magnet was tested under boiling liquid helium in a vertical dewar. The quench current showed very little dependence on ramp rate. The ac losses, measured by an electrical method, were fitted to straight line plots of loss/cycle versus ramp rate, thereby separating the eddy current and hysteresis components. These results were compared with calculated values, using parameters which had previously been measured on short samples of cable. Reasonably good agreement between theory and experiment was found, although the measured hysteresis loss is higher than expected in ramps to the highest field levels.**

Index Terms--**superconducting magnet, ac loss, dipole magnet, synchrotron, Rutherford cable, heavy ion.**

I. INTRODUCTION

G SI is planning a new heavy ion accelerator consisting of two superconducting synchrotron rings placed one above the other in the same tunnel [1], and ramping with a rise time of a few seconds. The lower ring, with a magnetic rigidity of 100T·m, will use magnets based on the Nuclotron design [2]. The upper ring was originally planned to be 200T·m and use magnets based on the RHIC design [3], but this ring has recently been increased to 300T·m. As a prototype for the original 200T·m ring, a 1m long model dipole has been built, based on the RHIC design, but with modifications to enable high ramp rates. The model has been successfully tested for quench behavior and ac losses at ramp rates up to 4T/s.

A previous paper [4] reported the details of magnet

construction and the initial quench test results. In a later test, the magnet was successfully ramped to 4T at 4 T/s without quenching. Also, the magnet was ramped for an extended period (40 minutes) to 4T at 2 T/s without quenching. In this paper, we briefly summarize the main construction features of the magnet and report the calculation and measurement of the hysteretic and eddy current energy loss.

II. CONSTRUCTION OF THE MODEL

A. Superconductor

The strand used for the cable has diameter 0.641 mm and J_c ~ 2900 A/mm^2 (5 T, 4.2 K, measured via transport current). The strand is coated with Staybrite. Two 25 μm thick, 8 mm wide stainless steel cores were inserted in the cable as it was formed. Other strand and cable parameters are given in Table I. The cable was insulated with two wraps of Kapton®, each 25 μm thick, and with 50% overlap of each wrap, with polyimide adhesive. A laser was used to cut cooling holes in the insulation on the thin edge of the insulated cable.

B. Magnet

This magnet (Fig. 1) used many designs and components from the RHIC and BNL/LHC programs but with magnet components made from insulators rather than metals when feasible. For example, the three wedges used in the coil were G11. The coils were collared with Kawasaki high-Mn stainless steel collars. The yoke laminations were 0.5 mm thick, low coercivity steel (H_c = 31 A/m) with 3.3% Si. Further details are given in [4].

III. TEST PROCEDURE

The magnet was tested in pool boiling He at 4.3 K without a beam tube. (Later, it will be tested in supercritical He at GSI.) There were two test periods. During the first, the magnet was in a dewar with a steel liner at a radius of 0.30 m. During the second, the magnet was tested in a dewar with a fiberglass liner. A fiberglass anticryostat was in the magnet bore during the second test.

IV. LOSS MEASUREMENTS

The energy loss was measured by recording the average voltage and current of the magnet over periods of 1/60 s. The cycle for a typical measurement is shown in Fig. 2. For each period, the energy was calculated as the VI product times the

G10 COIL SHIM
G10 COLLAR PACK STACKING RODS
G11 SLEEVES FOR RODS
SST YOKE TIE RODS
G11 COLLARING KEYS
G10 YOKE ALIGNMENT KEY
WELD BACKING STRIP
COLDMASS SHELL
SST COLLARS
G11 COIL WEDGES
HELIUM VENT SLOT
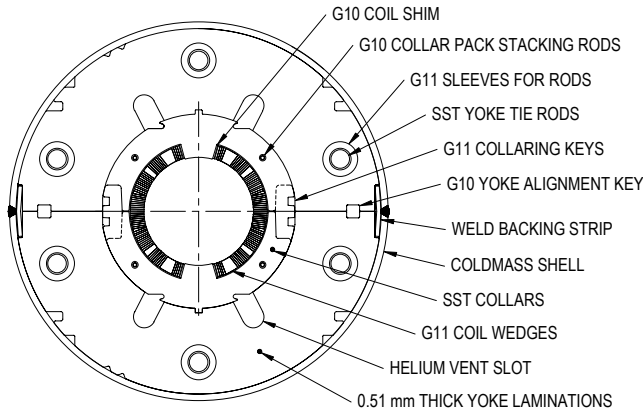0.51 mm THICK YOKE LAMINATIONS

Fig. 1. Cross section of the cold mass. The coil i.d. is 8 cm.

time between points. The magnet's voltage was measured by a precise voltmeter (HP3458A). The voltage taps on the magnet were placed on the superconducting leads, close to the coil (i.e., between the coil and the splice that joins the magnet's leads and the power supply's leads). The current was measured by a voltmeter of the same model, which recorded the output of a DCCT (Holec).

A typical energy loss for this magnet is ∼ 0.2% of the magnetic field energy, so considerable effort was invested in checking for and minimizing errors. The power supply control system was modified to minimize differences between the up ramp and the down ramp. The feedback circuit was adjusted to essentially eliminate overshoot. The control software generated smooth transitions between constant current and ramping. Each such transition accounted for typically 5% of the total ramp time. Dwell times at the minimum and maximum currents (typically 0.4 s and 0.2 s respectively) were minimized.

Two checks for offsets in the voltage were made with the power supply connected to the magnet but with the supply's reference input shorted. The first check was for DC offsets. There was no DC offset in the output voltage. Second, the effect of voltage errors was checked by programming the reference voltage to generate a fake, perfect current signal and
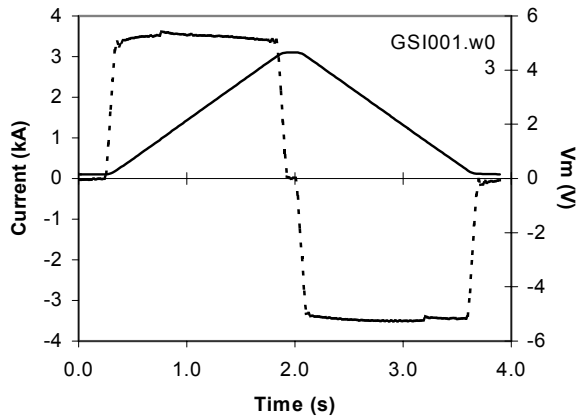

Fig. 2. V (dashed line) and I (solid line) for a typical energy loss measurement.

measuring an apparent energy loss. For a 2 T/s ramp to 5 kA, an apparent loss of 1 J was measured, much smaller than the magnet's measured loss under these same conditions, ∼80 J. The current offset is small, 0.2 A, and does not affect the measured energy loss.

Several other items should be mentioned. The measurement was not affected by the material used for the dewar liner. We checked that the resistance of the splice between the two coil halves did not contribute measurably to the energy loss. Initially, measurements were made at constant dI/dt. At the highest ramp rates, we implemented an algorithm to correct for the ∼ 8% drop in transfer function due to saturation at 4T so that the ramp would be at constant dB/dt. No significant difference was found between these measurements. The ramp rate quoted covers the entire time spent while ramping (including the smooth onset and rolloff of the ramp) but not the dwell times at high or low current. The AGS Booster Synchrotron, a possible source of perturbations of the 60 Hz AC signal, did not operate while these measurements were underway.

V. CALCULATION OF SUPERCONDUCTOR LOSS

We identify three different mechanisms for losses between strands in the cable:
- coupling via R_c in transverse field,
- coupling via R_a in transverse field,
- coupling via R_a in parallel field,

where R_c and R_a are the inter-strand resistances between crossover and adjacent strands. Formulae for the loss power from these coupling currents in linear field ramps are given in [5]. Here we consider the energy loss per cycle, i.e. mean loss power × cycle time.

Within each wire, there are two more loss mechanisms: coupling between the filaments and hysteresis within the filaments. Formulae for mean loss power are given in [5]. However, the hysteresis loss formula in [5] took no account of the transport current flowing in that cable because the short samples of cable being tested were not carrying current. From the critical state model it may be shown that the presence of a transport current I_t increases the instantaneous hysteresis loss power by a factor $(1+i^2)$ where $i = I_t/I_c$. For magnet losses, we must therefore integrate this factor over the field variation during a ramp at each point in the magnet. In [5] we assumed the following variation of J_c with field:

$$J_c(B) = \frac{J_o B_o}{B + B_o} + A_o + A_1 B \tag{1}$$

Unfortunately, this expression is cumbersome to integrate, so we have instead used the simpler Kim Anderson expression.

$$J_c(B) = \frac{J_o B_o}{B + B_o} \tag{2}$$

to calculate an additional hysteresis loss per cycle of

$$\Delta Q_{hie} = \frac{d_f I_e^2}{9\pi} \frac{(3B_e^4 + 4B_e^3 B_o - 3B_i^4 - 4B_i^3 B_o)}{J_o B_o B_e^2 \lambda_c \lambda_w \lambda_f (4ab)^2} \tag{3}$$

where B_i, I_i and B_e, I_e are the local fields and magnet currents at injection and extraction; other factors are as listed in Table 1.

With the above formulae, losses are calculated by integration over the two dimensional field pattern, using a simple spreadsheet, which divides the winding cross section into sectors of size 1° azimuthally and 2 mm radially. The magnet length is adjusted to give the actual cable volume, but of course this method only gives an approximate answer for the end turns.

VI. CALCULATION OF IRON LOSS

The hysteresis losses of the yoke material (EBG M250-50A) were determined with a ring sample measurement. The standard ring sample size was used (outer diameter 114mm, inner diameter 76mm, height 12mm). Special care was taken to prevent eddy currents by using a laminated sample, by keeping a constant low ramp rate dB/dt, and by waiting for the eddy currents to die out. Before each measurement the sample was demagnetized. Unipolar hysteresis cycles starting at $-H_c$ were measured for different excitations. Fig. 3a shows the measured specific iron hysteresis losses vs. the iron B-field. An almost quadratic dependence for the measured range was determined. Higher iron B-fields could not be measured because of the limited cooling capability of our ring sample testing device.
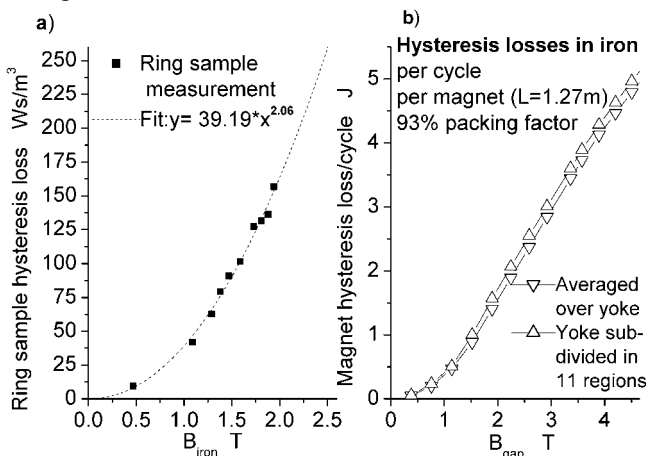

Fig 3. a) Measured ring sample iron hysteresis losses b) Calculated magnet iron hysteresis losses, using the measurement of the ring.

The measured BH-curve was then used in a 2d OPERA FEM calculation. In a first step the average B-field over the full yoke cross section was determined for different excitations of the magnet. Secondly the measured ring sample hysteresis losses and the average B-field were combined to calculate the appropriate iron hysteresis losses in the magnet cross section per unit length of the magnet. By using the natural subdivision of the FE model into regions the calculation was refined later on. Fig. 3b shows the losses per cycle vs. the B-field in the gap, calculated for the model yoke, which has a length of 1.27m and a filling factor of 93%.

VII. CALCULATED LOSSES COMPARED WITH MEASUREMENTS

Parameters used in the calculation are listed in Table 1. The inter-strand resistances were obtained from VI measurements on short samples of cable [6]. Values for the critical current fitting coefficients and coupling time constant are deduced from measurements of magnetization on individual wires in fields ramping at various rates [7].

TABLE 1
PARAMETERS USED IN THE LOSS CALCULATION

cable half width	a = 4.87mm
cable half thickness	b = 5.83mm
cable twist pitch	p = 74mm
number of strands	N = 30
filling factor of cable in winding	λ_c = 0.826
filling factor of wire in cable	λ_w = 0.872
matrix ratio	mat = 2.25
filling factor of filaments in wire	λ_f = 0.308
wire twist pitch	p_w = 4.0mm
filament diameter	d_f = 6.0μm
crossover resistance	R_c = 60mΩ
adjacent resistance	R_a = 74μΩ
wire transverse resistivity	$\rho_t = 2.14.10^{-10}$Ωm
wire coupling time constant	τ = 1.19ms
Kim Anderson	$J_o = 3.85.10^{10}$A.m^{-2}
Kim Anderson	B_o = 0.130 Tesla
Kim Anderson	$A_0 = 4.35.10^9$A.m^{-2}
Kim Anderson	$A_1 = -5.9.10^8$A.m^{-2}T^{-1}

Fig. 4 shows some typical results of the calculation, together with the experimental measurements.
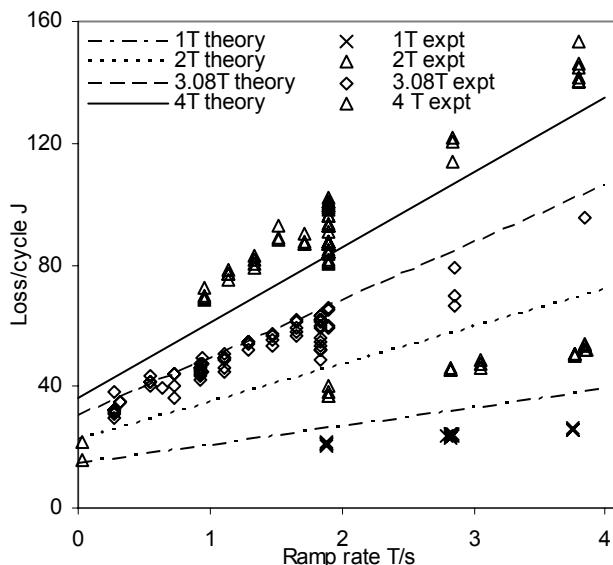

Fig 4. Calculated and experimental data of loss per cycle versus dB/dt for various values of maximum field

In order to compare the calculation with the totality of experimental data, we fit the experimental points to straight lines and compare the gradients (eddy current loss) and intercepts (hysteresis loss) with calculation. Fig. 5 shows the gradient plot. The two calculated lines come from different assumptions about the cable coupling loss via R_a in transverse field. As noted in [7], this loss can be increased by up to a factor 3 if the R_a contact is predominantly at the edge of the

cable and, as noted in [6], we have seen some indication that R_a is lower at the edge than in the centre. Thus we choose factors of 1.5 or 2 as an intermediate between the two extremes. From Fig. 5, it would appear that the edge concentration gets stronger at high fields, perhaps an effect of the increasing forces.
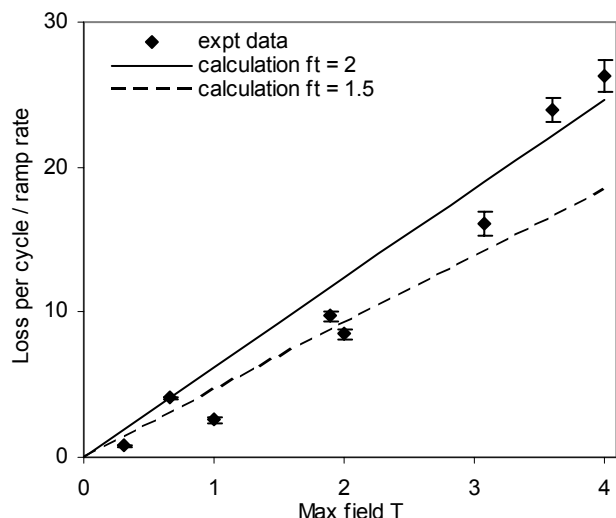

Fig 5. Experimental and calculated gradient of (loss per cycle vs. ramp rate) vs. maximum field (bars show error in fitting experimental data).
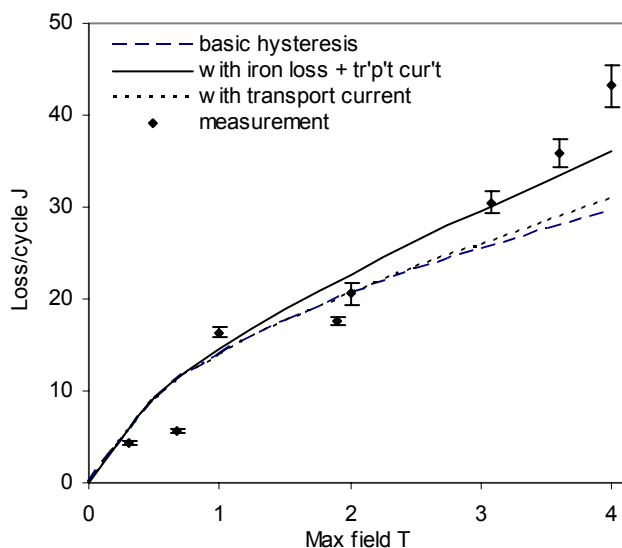

Fig 6. Calculated and experimental data of hysteresis loss per cycle (intercept of loss vs. dB/dt plots, bars show error in fitting experimental data).

Secondly we plot the intercept of the plots at zero ramp rate, which is the hysteresis loss per cycle. Theoretically, this loss comprises three terms: the superconductor hysteresis loss, the enhancement caused by transport current and the iron loss. Fig 6 shows each of the calculated terms. It may be seen that the transport current correction has not made much difference. The iron hysteresis makes an increasing contribution at high fields, but does not fully explain the upward curvature of the experimental data. Nevertheless, the general level of agreement is reasonably good.

VIII.   CONCLUSIONS.

Even in the fastest sweeps of 4T/s to 4T, our model dipole has shown no effect of ramp rate on quench current. AC losses show the expected behaviour of a hysteresis component plus a component comprising coupling and eddy currents, which increases linearly with ramp rate. Using a set of parameters derived from measurements on short samples of wire and cable, we have calculated hysteresis and rate dependent components of loss which are in very reasonable agreement with the measured losses. The rate dependent losses seem to confirm that our conductor has an adjacent resistance R_a which is lower at the edge of the cable than in the centre and that, perhaps, this effect gets stronger at high fields, i.e. at high stresses. Hysteresis loss is generally as predicted, but the experimental plots show a somewhat stronger upward curvature at high fields; we have no explanation for this.

Overall, the lack of an effect of ramp rate on quench current and the rather low and predictable ac losses show that this method of coil construction is very suitable for fast ramping accelerator magnets.

REFERENCES

[1] G. Moritz, "Superconducting magnets for the 'International Accelerator Facility for Beams of Ions and Antiprotons' at GSI," *IEEE Trans. Appl. Superconductivity*, vol. 13, no. 2, pp. 1329–1331, June 2003.

[2] A.D. Kovalenko, N.N. Agapov, A.M. Donyagin, H.G. Khodzhibagiyan, G.L. Kuznetsov, G. Moritz, G. Hess, J. Kaugerts, E. Fischer and C. Muehle, "Superferric model dipole magnet with the iron yoke at 80K for the GSI future fast cycling synchrotron," *IEEE Trans. Appl. Superconductivity*, vol. 13, no. 2, pp. 1335–1337, June 2003.

[3] M. Anerella, J. Cozzolino, J. Escallier, G. Ganetis, A. Ghosh, R. Gupta, M. Harrison, A. Jain, S. Kahn, E. Killian, W. Louie, A. Marone, J. Muratore, S. Plate, M. Rehak, W. Sampson, J. Schmalzle, R. Thomas, P. Thompson, P. Wanderer, E. Willen, "The RHIC magnet system," *Nucl. Inst. Meth. A*, vol. 499, pp. 280–315, 2003.

[4] P.Wanderer, M. Anerella, G. Ganetis, A. Ghosh, P. Joshi, A. Marone, J. Muratore, J. Schmalzle, R. Soika, R. Thomas, J. Kaugerts, G. Moritz, W. Hassenzahl, M. N. Wilson, "Initial test of a fast-ramped superconducting model dipole for GSI's proposed SIS200 accelerator," presented at the 2003 Particle Accelerator Conference, Portland OR USA, May 12-16, 2003, available:
http://warrior.lbl.gov:7778/pacfiles/papers/WEDNESDAY/AM_POSTER/WPAB054/WPAB054.PDF

[5] M.N. Wilson , G. Moritz , M. Anerella , G. Ganetis, A.K. Ghosh, W.V. Hassenzahl , A. Jain, P. Joshi, J. Kaugerts, C. Muehle, J. Muratore, R. Thomas, G. Walter, P. Wanderer, "Design studies on superconducting cosθ magnets for a fast pulsed synchrotron," *IEEE Trans Appl. Superconductivity*, vol. 12, no. 1, pp. 313–316, March 2002.

[6] R. Soika, M. Anerella, A.K. Ghosh, P. Wanderer, M.N. Wilson, W.V. Hassenzahl, J. Kaugerts, and G. Moritz, "Inter-strand resistance measurements in cored Rutherford cables," *IEEE Trans. Appl. Superconductivity*, vol. 13, no. 2, pp. 2380–2382, June 2003.

[7] M.N. Wilson, A.K. Ghosh, B. ten Haken, W.V. Hassenzahl, J. Kaugerts, G. Moritz, C. Muehle, A. den Ouden, R. Soika, P. Wanderer, W. A. J. Wessel, "Cored Rutherford cables for the GSI fast ramping synchrotron," *IEEE Trans. Appl. Superconductivity*, vol. 13, no. 2, pp. 1704–1706, June 2003.